Journal of ELECTRONIC MATERIALS, Vol. 48, No. 8, 2019
https://doi.org/10.1007/s11664-019-07331-2

Tunable Non-linear Optical, Semiconducting and Dielectric Properties of $In_{1-x}Mn_xSe$ Thin Films

S.A. GAD,[1,3] G.M. MAHMOUD,[2] and A. ABDEL MOEZ[2]

1.—Semiconductor Laboratory, Physical Research Division, Solid State Physics Department, National Research Centre, 33 El-Bohouth St., Dokki, Giza 12622, Egypt. 2.—Solid State Electronics Laboratory, Physical Research Division, Solid State Physics Department, National Research Centre, 33 El-Bohouth St., Dokki, Giza 12622, Egypt. 3.—e-mail: samiagad2000@yahoo.com

$In_{1-x}Mn_xSe$ (x = 0, 0.05, 0.1 and 0.15) thin films were evaporated by using the thermal evaporation technique. Both dispersion energy (E_d) and oscillating energy (E_o) were determined. The values of lattice dielectric constant (ε_L) and free carrier concentration/effective mass) (N/m^*) were calculated. On the other hand, the values of the first order of moment (M_{-1}), the third order of moment (M_{-3}) and static refractive index (n_o) were determined. The dielectric loss (ε') and dielectric tangent loss (ε'') for these films increased with photon energy and had the highest value near the energy gap E_g. Also, the same behavior was noticed for the real part of optical conductivity (σ_1) and imaginary part of optical conductivity (σ_2), the relation between Volume Energy Loss Function (*VELF*) and Surface Energy Loss Function (*SELF*) was determined. The Linear optical susceptibility ($\chi^{(1)}$) increased with photon energy for all compositions. The nonlinear optical parameters such as nonlinear refractive index (n_2), the third-order nonlinear optical susceptibility ($\chi^{(3)}$) and nonlinear absorption coefficient (β_c), were determined theoretically. Both the electrical susceptibility (χ_e) and relative permittivity (ε_r) increased with photon energy and had the highest value near the energy gap. The semiconducting results such as density of the valence band, conduction band, and Fermi level position (E_f) were calculated.

Key words: $In_{1-x}Mn_xSe$ thin films, dielectric results, non-linear optical properties, semiconducting and electronic results

INTRODUCTION

An $A_{III}B_{VI}$ semiconductor such as $Ga_{1-x}Mn_xS$.[1–3] $Zn_{1-x}Mn_xSe$,[4] and finally $In_{1-x}Mn_xSe$[5–7] had been studied widely because of their applications such as in solar energy conversion,[8–12] infrared devices,[9] lasers,[9] and photovoltaic applications[13] diodes.[14] The structural and physical properties of InSe were investigated[15–18] InSe thin films had a polycrystalline structure after heat treatment[19–22] The optical properties of InSe thin films were studied,[23–29] it was found that InSe samples had a direct energy gap of 1.35 ± 0.02 eV.[24] 1.10 eV,[25] (2.5 to 3.34 eV)[26] and the values of (1.7, 1.2 and 1.1 eV).[17] The electrical and dielectric studies for InSe thin films and crystals were studied[30–35] the ac conductivity was decreased with frequency for InSe.[30] The temperature affected on ac conductivity[31–33] as a result of its strong electron interaction with holes.[36] On the other hand, MnSe had been studied widely and it was noticed that MnSe crystals had a hexagonal structure with a lattice constant of (a = 5.462 Å) and (a = 3.63 Å; c = 5.91 Å).[37–39] The optical properties of MnSe thin films had been studied,[40–42] MnSe had an energy gap (1.13–1.25 eV).[40,41] The electrical and dielectric properties had been investigated[42–44] the electrical resistivity of MnSe decreased with temperature.[44] Moreover,

(Received January 28, 2019; accepted May 25, 2019; published online June 3, 2019)

the transport properties of $In_{1-x}Mn_xSe$ had been studied[7,45–48] the energy gap and structure dependence on the composition of $In_{1-x}Mn_xSe$ thin films and bulk materials had been studied[49,50] and these thin films had an amorphous structure,[49] the energy gap increased with the x values for both thin films and bulk material.[50] The aim of the present work is studying the effect of the composition on dielectric loss (ε') and dielectric tangent loss (ε'') both of real and imaginary parts of optical conductivity (σ_1 and σ_2) respectively, electrical susceptibility ($\chi_{(e)}$), linear optical susceptibility ($\chi^{(1)}$), the non-linear optical results such as nonlinear refractive index (n_2), nonlinear absorption coefficient (β_c), non-optical susceptibility ($\chi^{(3)}$), dielectric results and finally electronic properties such as Fermi level position (E_f) and density of both of valence conduction band (N_v) and conduction band (N_c) of $In_{1-x}Mn_xSe$ thin films.

EXPERIMENTAL WORKS

Bulk ingot materials of the ternary $In_{1-x}Mn_xSe$ (x = 0, 0.05, 0.1, and 0.15) were prepared by the direct fusion method of pure (5 N) individual elements in stoichiometric proportions. The mixture was contained in cleaned silica tubes sealed under vacuum pressure of 10^{-5} kPa. The sealed tubes were baked in a high-temperature furnace at 1100°C for 72 h. Thin films of $In_{1-x}Mn_xSe$ were deposited at room temperature by thermal evaporation under vacuum of 10^{-5} kPa. The deposition process was carried out on cleaned glass substrates. Transmittance (T) and reflectance (R) of the as-deposited thin films on precleaned glass substrates were determined at normal incidence using a Jasco (V-570) spectrophotometer from 500 to 2500 nm to determine some optical parameters of $In_{1-x}Mn_xSe$. The optical measurements were carried out at room temperature. The thickness of the evaporated films was determined by a quartz thickness monitor which is attached with the coating unit and confirmed by multiple-beam interferometers (the technique of multiple-beam interferometry is based upon situating two surfaces of high reflectivity in close proximity and using a lens to converge beams which have undergone multiple reflections between the surfaces).

RESULTS AND DISCUSSION

Optical Results

The structure of these thin films with different compositions had an amorphous structure as reported in previous work.[49] The optical transmittance (T) and reflectance (R) were measured and discussed in previous work.[49] The single oscillator theory was expressed by the Wemple–DiDomenico relationship:[51]

$$n^2(E) - 1 = \frac{E_o \cdot E_d}{E_o^2 - E^2}, \quad (1)$$

where n is the refractive index values of these samples, which is determined in previous work,[49] E is the photon energy, E_o is the oscillator energy and E_d is the dispersion energy. The values of E_o and E_d for all samples are shown in Table I. Figure 1 shows the relation of n^2 and λ^2 to determine the effective mass ratio with the carrier concentration using the following equation:[52]

$$n^2 - k^2 = \varepsilon_L - \left(\frac{eN}{4\pi c^2 \varepsilon_o m^*}\right)\lambda^2, \quad (2)$$

where ε_L is the lattice dielectric constant, ε_o is the permittivity of free space, e is the charge of electron, n, k is the linear refractive index and the absorption index of these films, respectively, which were determined in previous work,[49] N is the free carrier concentration for $In_{1-x}Mn_xSe$ films and c is the speed of light so the values of N/m^* are shown in table I. From this table, it was noticed that the value of x affected the ratio of N/m^*, the access of Mn for the access of electrons. The values of the first order of moment (M_{-1}) and the third order of moment (M_{-3}) are derived from the relations:[52]

$$E_o^2 = \frac{M_{-1}}{M_{-3}} \quad (3)$$

$$E_d^2 = \frac{M_{-1}^3}{M_{-3}} \quad (4)$$

Table I shows the values of M_{-1} and M_{-3} for these thin films. The oscillator strength (f) which was calculated as follows:[53]

$$f = E_o \cdot E_d \quad (5)$$

The values of the f are shown in Table I. Another important parameter depends on both E_o and E_d is that static refractive index (n_o) which was determined using the following equation:[54]

$$n_o = \left[\left(E_d/E_o\right) + 1\right]^{0.5}. \quad (6)$$

The values of n_o for all these samples are shown in Table I.

Dielectric, Optical Conductivity and Linear Optical Susceptibility Results

Figure 2 represents the relation between $(n^2 - 1)$ 1 versus $h\nu$ for these thin films. It is shown that $(n^2 - 1)^{-1}$ increases as Mn content increases. The increase in refractive index is explained on the basis of the Lorentz–Lorentz relation.[55] This relation reports that the larger atomic radius, the greater

Table I. The determined values of $In_{1-x}Mn_xSe$ thin films such as lattice dielectric constant εL, Oscillation energy E_o, Dispersion energy E_d, first order of moment M_{-1}, third order of moment M_{-3}, Field strength (*f*), static refractive index (n_o), (N/m^*), density of conduction band N_c (cm^{-3}), density of valence band N_v (cm^{-3}) and Fermi level position

Sample	Lattice dielectric constant ε_L	Oscillation energy E_o (eV)	Dispersion energy E_d (eV)	$M-1$ (eV)	$M-3$ (eV)	Field strength (*f*) $(eV)^2$	n_o	N/m^*	Nc/m_h^*	N_V	Fermi level Position (eV)
InSe	02.00	3.14	4.22	3.64	2.05	13.25	1.53	1.1×10^{49}	9.3×10^{20}	4.1×10^{21}	0.24
$In_{0.05}Mn_{0.95}Se$	03.00	3.20	4.30	3.71	2.07	13.76	1.53	1.2×10^{49}	9.3×10^{20}	3.6×10^{21}	0.23
$In_{0.1}Mn_{0.9}Se$	13.00	3.36	4.50	3.89	2.12	15.12	1.54	1.5×10^{49}	9.3×10^{20}	3.8×10^{21}	0.21
$In_{0.15}Mn_{0.85}Se$	10.00	3.04	4.80	4.04	2.19	16.32	1.55	1.7×10^{49}	9.3×10^{20}	3.8×10^{21}	0.23

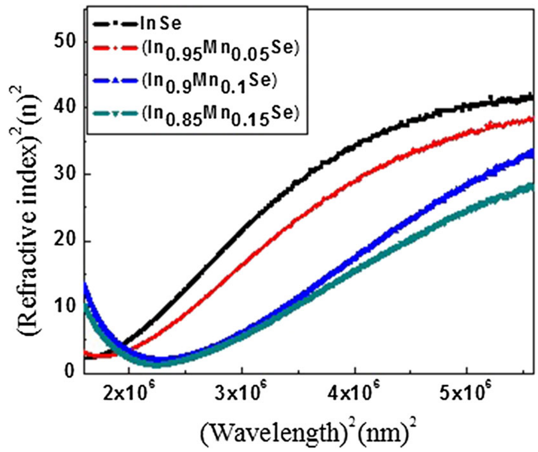

Fig. 1. Relation between n^2 and λ^2 for $In_{1-x}Mn_xSe$ (x = 0, 0.05, 0.1 and 0.15).

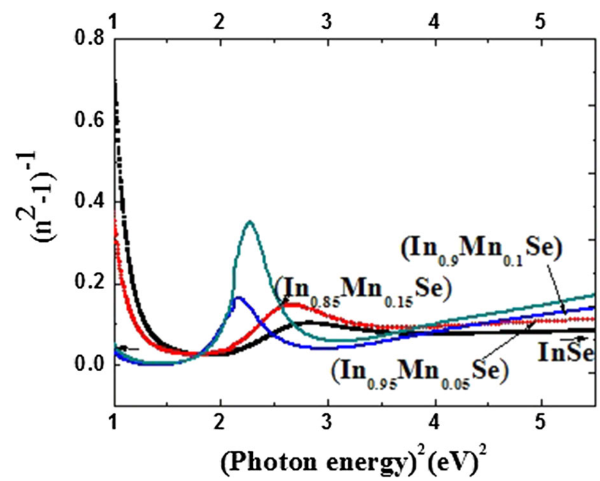

Fig. 2. $(n^2-1)^{-1}$ vs. $(h\nu)^2$ for $In_{1-x}Mn_xSe$ (x = 0, 0.05, 0.1 and 0.15).

polarizability and then the larger refractive index. Also In (193 Pm) is replaced by Mn (197 Pm) atoms and the polarizability and afterward the refractive index increases. The dependence of dielectric constant on the photon energy suggests that some interactions between photons and electrons in the films are produced in this energy range. These interactions affect the shapes of the real and imaginary parts of the dielectric constant, and they are the reason for the formation of peaks in the dielectric spectra which depends on the material type. The dielectric loss (ε') and dielectric tangent loss (ε'') for these films were calculated as follows:[56]

$$\varepsilon' = (n^2 + k^2), \tag{7}$$

$$\varepsilon'' = \left[(n^2 + k^2)^2 - (n^2 - k^2)^{0.5}\right]. \tag{8}$$

Figure 3a and b show ε' and ε'' versus $h\nu$ for $In_{1-x}Mn_xSe$ films. From this Fig., it was seen that

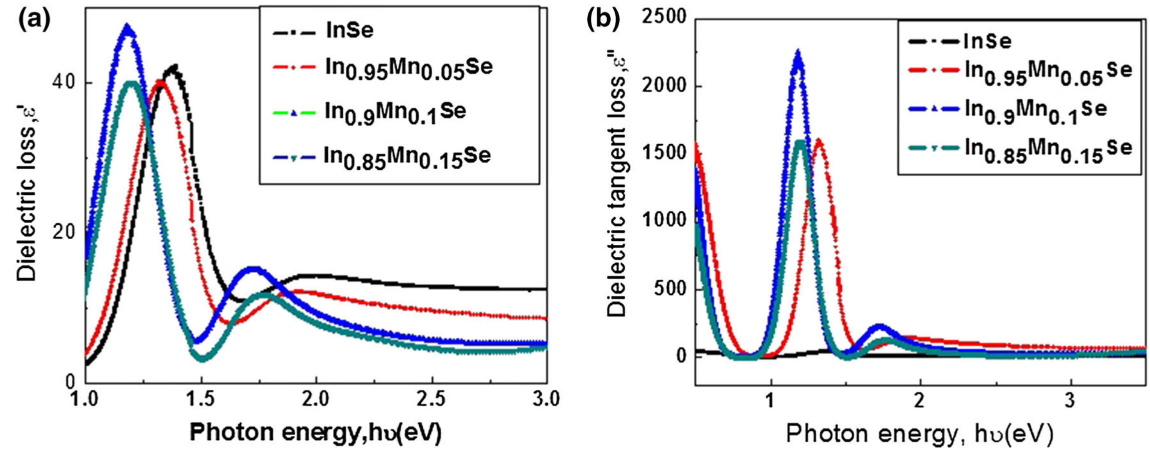

Fig. 3. (a) Dielectric loss as a function of $h\nu$ (b) dielectric tangent loss and $h\nu$ for $In_{1-x}Mn_xSe$ (x = 0, 0.05, 0.1 and 0.15).

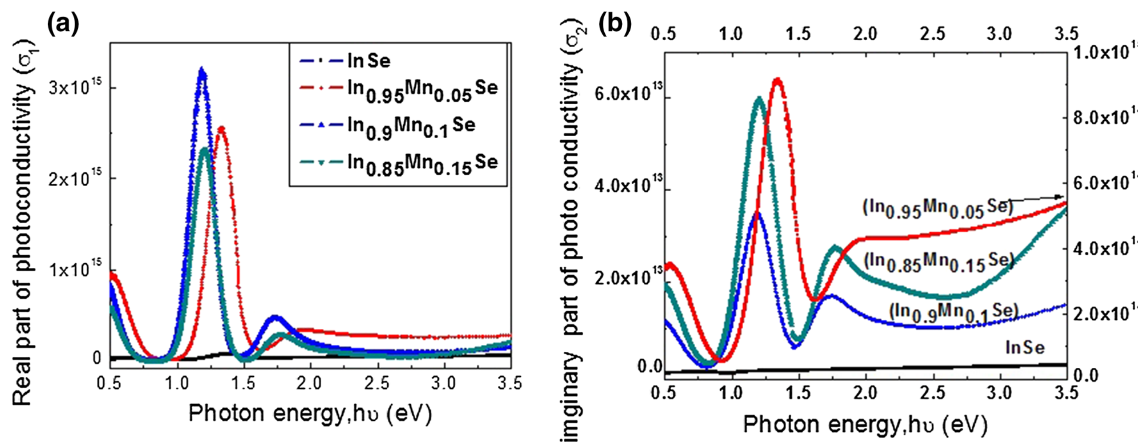

Fig. 4. (a) Relation between real part of optical conductivity $h\nu$. (b) Dielectric imaginary part of optical conductivity and $h\nu$ for $In_{1-x}Mn_xSe$ (x = 0, 0.05, 0.1 and 0.15).

both ε' and ε'' decreased with $h\nu$ for all studied samples and the peak maximum values position decreased with increasing Mn content; this is due to the increase of electron motilities with x values. The optical conductivity was calculated from the following equations:[57]

$$\sigma_1 = \left(\frac{\varepsilon'' \cdot c}{2\lambda}\right), \tag{9}$$

$$\sigma_2 = \frac{(1-\varepsilon') \cdot c}{4\lambda}. \tag{10}$$

Figure 4a and b show both σ_1 and σ_2 dependence on $h\nu$ for these films. The behavior of both σ_1 and σ_2 for all these studied films is the same with $h\nu$ and increase with $h\nu$ for all these samples. The values of Volume Energy Loss Function (VELF) and Surface Energy Loss Function (SELF) for these films were determined optically as follows:[52]

$$\mathrm{VELF} = \frac{\varepsilon''}{\varepsilon'^2 + \varepsilon''^2}, \tag{11}$$

$$\mathrm{SELF} = \frac{\varepsilon''}{(\varepsilon'+1)^2 + \varepsilon''^2}. \tag{12}$$

The relation between *VELF*/*SELF* for these thin films is shown in Fig. 5. Linear optical susceptibility ($\chi^{(1)}$) describes the response of the material to an optical wave-length χ^1 and was determined using the following relation[58]:

$$\chi^{(1)} = \frac{(n^2-1)}{4\pi}. \tag{13}$$

The relation between χ^1 and $h\nu$ for $In_{1-x}Mn_xSe$ thin films is shown in Fig. 6. From this figure it was seen that the linear optical susceptibility ($\chi^{(1)}$) increased with $h\nu$; this means that there is a

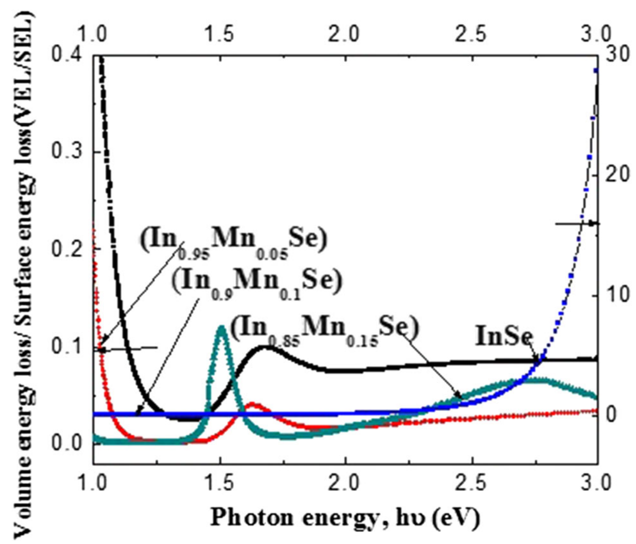

Fig. 5. (VELF/SELF) against hν for $In_{1-x}Mn_xSe$ (x = 0, 0.05, 0.1 and 0.15).

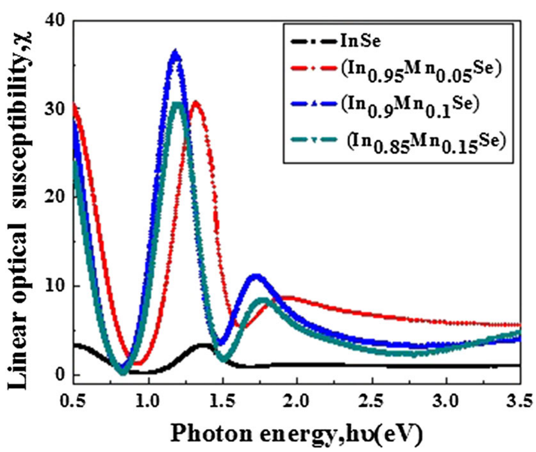

Fig. 6. Relation between Linear optical susceptibility and hν for $In_{1-x}Mn_xSe$ (x = 0, 0.05, 0.1 and 0.15).

possibility of wide change in optical properties by a slight change in composition for these samples.

Nonlinear Optical Properties

An important parameter of the non-linear optical parameters is that the nonlinear refractive index (n_2) which can be explained as when light with high intensity propagates through a medium, this causes nonlinear effects[59] and n_2 was determined from the following simple equation:[60,61]

$$n_2 = \left(\frac{12\pi\chi^{(3)}}{n_o}\right)^{0.5}. \qquad (14)$$

The dependence of n_2 on wavelength for $In_{1-x}Mn_xSe$ thin films is shown in Fig. 7. The values of n_2 decrease with wavelength for all these studied samples. An important parameter to assess

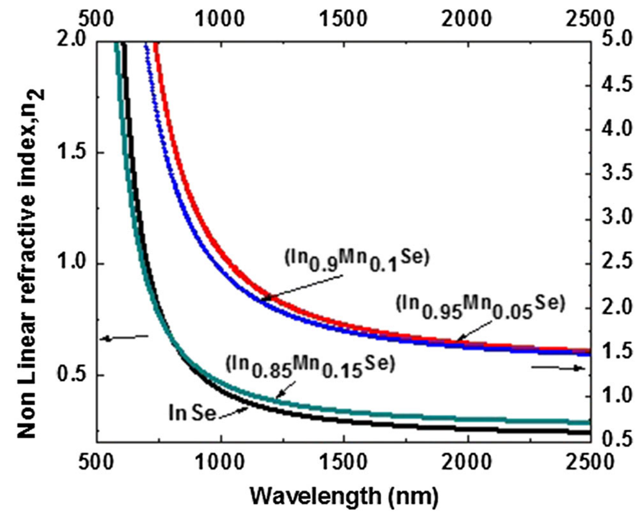

Fig. 7. Non Linear refractive index as a function of wavelength for $In_{1-x}Mn_xSe$ (x = 0, 0.05, 0.1 and 0.15).

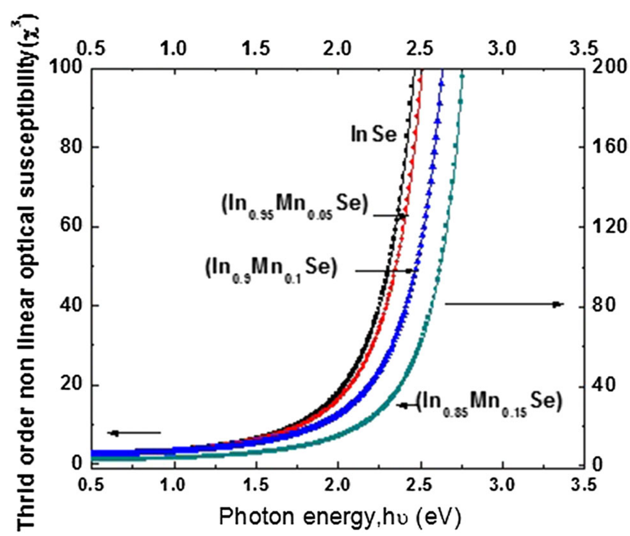

Fig. 8. Relation between third order nonlinear optical susceptibility and $h\nu$ for $In_{1-x}Mn_xSe$ (x = 0, 0.05, 0.1 and 0.15).

the degree of nonlinearities is the third order nonlinear optical susceptibility ($\chi^{(3)}$) which was determined using the following equation[62]:

$$\chi^{(3)} = A\left[\frac{E_o \cdot E_d}{4\pi(E_o^2 - (h\nu)^2)}\right]^4, \qquad (15)$$

where A is a quantity that is assumed to be frequency independent and nearly the same for all materials = 1.7 × 10^{-10} e.s.u.[62] The third order nonlinear optical susceptibility ($\chi^{(3)}$) dependance on photon energy for $In_{1-x}Mn_xSe$ thin films with different x values is shown in Fig. 8. It was noticed that the behavior of χ^3 is the same for all the studied samples; the values of χ^3 increase with $h\nu$ and this is due to when $h\nu$ increased the deflection of the incident light beam increase. On the other hand, the

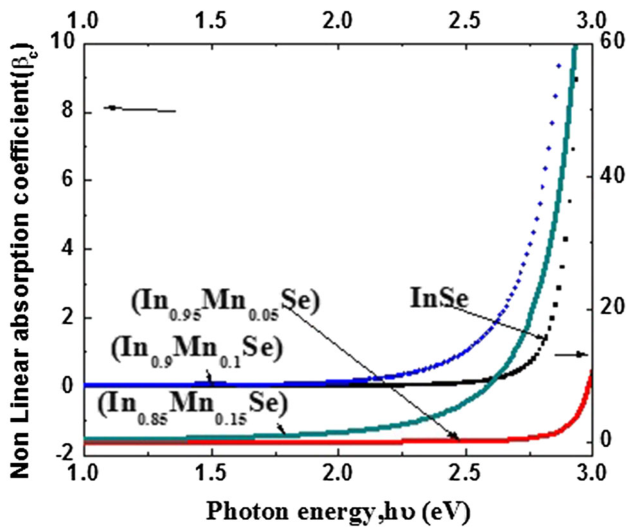

Fig. 9. Nonlinear absorption coefficient as a function of $h\nu$ for $In_{1-x}Mn_xSe$ (x = 0, 0.05, 0.1 and 0.15).

non-linear absorption coefficient (β_c) was determined as follows:[63]

$$\beta_c = \frac{48 \cdot \pi^3 . \chi^{(3)}}{n^2 \cdot c \cdot \lambda}. \tag{16}$$

Figure 9 shows the influence of hν on β_c. It is observed that the values of β_c increase with $h\nu$ for all these samples as shown in Fig. 9. Because of the higher values of $h\nu$, the large numbers of excited electrons overcome the band gap.

Electrical Results

Electrical susceptibility ($\chi_{(e)}$) was estimated using the following relation:[64]

$$\chi_{(e)} = \frac{(n^2 - k^2 - \varepsilon_o)}{4\pi}. \tag{17}$$

Figure 10 shows the electrical susceptibility ($\chi_{(e)}$) dependence on $h\nu$ of these investigated samples. From this figure, it is clear that the values of χ_e increase with $h\nu$; this is due to the electron mobility increase with $h\nu$. The relative permittivity ε_r was calculated using the following relation:[65]

$$\varepsilon_r = (\chi_e + 1) \tag{18}$$

The relation between relative permittivity (ε_r) and wavelength for $In_{1-x}Mn_xSe$ thin films with different x values is shown in Fig. 11. It is clear that the values of ε_r increase with $h\nu$ for all these samples; this could be attributed to the electron mobility increase with $h\nu$.

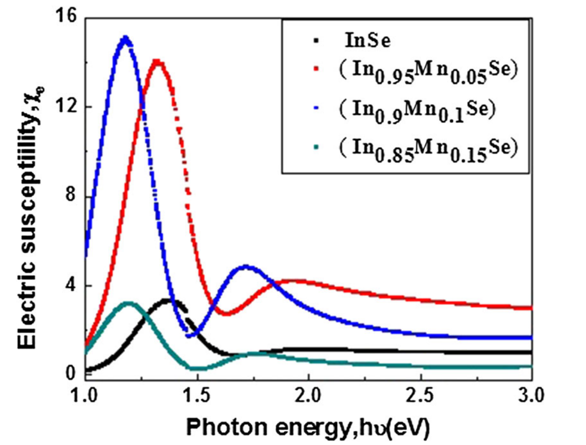

Fig. 10. Relation between electrical susceptibility and $h\nu$ for $In_{1-x}Mn_xSe$ (x = 0, 0.05, 0.1 and 0.15).

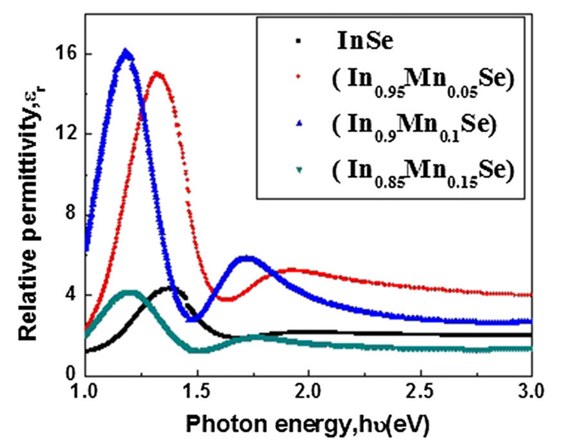

Fig. 11. Relative permittivity versus $h\nu$ for $In_{1-x}Mn_xSe$ (x = 0, 0.05, 0.1 and 0.15).

Semiconducting and Electronic Results

The density of states (DOS) of a system describes the number of states per interval of energy at each energy level available to be occupied. The N_v and N_c play a very important rule of examination for the linear optical transition and non-linear optical properties. The N_v and N_c were calculated as follows:[66]

$$N_v = 2\left[{(2\pi m_h^* KT)}/{h^2}\right]^{3/2}, \tag{19}$$

$$N_c = 2\left[{(2\pi m_e^* KT)}/{h^2}\right]^{3/2}, \tag{20}$$

where N_v and N_c were the density of states for both valence and conduction bands, respectively, effective mass of electrons m_e^* (InSe) = 0.14[67] m_e^* (MnSe (= 0.15[68] effective mass of holes m_h^* (InSe) = 0.37[67] and K is a Boltzmann constant. The determined values for both N_v, N_c are shown in table I. Another important factor that was determined theoretically is the position of the Fermi level:[62]

$$E_f = \left(\frac{KT}{q}\right) \cdot \ln\left(N_c/N_v\right). \quad (21)$$

The values of the Fermi level position for these investigated thin films are shown in Table I.

CONCLUSION

The values of E_d and E_o for $In_{1-x}Mn_xSe$ increased with increasing Mn content and had the values (4.22 to 4.80 eV) and (3.14 to 3.40 eV), respectively. The values of (N/m^*) increased with increasing x values. The values of M_{-1} and M_{-3} also increase with increasing Mn concentration. n_o increased slightly with Mn content. The refractive index increased with increasing Mn content due to the difference in atomic radius of In and Mn. The ε' and ε'' increased with $h\nu$; the maximum values decreased with increasing Mn content due to the increase of electron mobility with increasing Mn ratio. The refractive index increased with increasing Mn content due to the difference in atomic radius of In and Mn. The χ^1 increased with $h\nu$ for all compositions. The values of n_2 increased with λ for all these samples while χ^3 increased with $h\nu$. This means that these samples had a high ability to change their optical properties by changing wavelength and applied field. The non-linear absorption coefficient (β_c) increased with $h\nu$ for these samples, also both χ_e and ε_r increased with $h\nu$ and had the highest value near the energy gap. The composition values x affected the values of both N_v and N_c while E_f was affected slightly with the composition values x.

REFERENCES

1. C. Fuller, A. Douglas, J. Garner, T.M. Pekarek, I. Miotkowski, and A.K. Ramdas, *Phys. Rev. B* 65, 195211 (2002).
2. M. Pekarek, M. Duffy, J. Garner, B.C. Crooker, I. Miotkowski, and A.K. Ramdas, *J. Appl. Phys.* 87, 6448 (2000).
3. J.L. Tracy, G. Franzese, A. Byrd, J. Garner, and T.M. Pekarek, *Phys. Rev B* 72, 165201 (2005).
4. D. Segev and S.-H. Wei, *Phys. Rev. B* 70, 184401 (2004).
5. T.M. Pekarek, D.J. Arenas, I. Miotkowski, and A.K. Ramdas, *J. Appl. Phys.* 97, 10M106 (2005).
6. D. Meda, J.H. Blackburn, L. Maxwell, J. Garner, T.M. Pekarek, I. Miotkowski, and A.K. Ramdas, *J. Appl. Phys.* 105, 07C521 (2009).
7. V.V. Slyn'ko, A.G. Khandozhko, Z.D. Kovalyuk, V.E. Slyn'ko, A.V. Zaslonkin, M. Arciszewska, and W. Dobrowolski, *Thin Solid Films* 258, 86 (1995).
8. M. Parlak, C. Ercelebi, I. Gunal, Z. Salaeva, and K. Allakherdiev, *Thin Solid Films* 258, 86 (1995).
9. S. Gopal, C. Viswanathan, B. Karunajaran, D. Mangalaraj, and S.K. Narayandas, *Cryst. Res. Technol.* 40, 557 (2005).
10. N. Benramdane, A. Bousidi, H. Tabet-Derraz, Z. Kebbab, and M. Latreche, *Microelectron. Eng.* 51, 645 (2000).
11. J.S. Somghera, I.D. Agarwal, and L.B. Shaw, *J. Optoelectron. Adv. Mater.* 3, 627 (2001).
12. J. Palm, V. Probst, and H. Karg Franz, *Sol. Energy* 77, 757 (2004).
13. Z.D. Kovalyuk, O.M. Sydor, and V.V. Netyaga, *Semicond. Phys. Quantum Electron. Optoelectron.* 7, 360 (2004).
14. G. Micocci and A. Tepore, *Sol. Energy Mater.* 22, 215 (1991).
15. B. Kobbi and N. Kesri, *Vacuum* 75, 177 (2004).
16. F.I. Mustafa, S. Gupta, N. Goyal, and S.K. Tripathi, *Phys. B* 405, 4087 (2010).
17. P. Matheswaran, R. Saravana Kumar, and R. Sathyamoorthy, *Vacuum* 85, 820 (2011).
18. A.A.A. Darwish, M.M. El-Nahass, and M.H. Bahlol, *Appl. Surf. Sci.* 276, 210 (2013).
19. S. Boolchandani, S. Srivastava, and Y.K. Vijay, *J. Nanotechnol.* 2018, 9380573 (2018).
20. K.S. Chaudhari, Y.R. Toda, A.B. Jain, and D.N. Gujarathi, *Adv. Appl. Sci.* 2, 84 (2011).
21. M. Teenaa, A.G. Kunjomana, K. Ramesh, R. Venkatesh, and N. Naresh, *Sol. Energy Mater. Sol. Cells* 166, 190 (2017).
22. A.I. Hirohata, J.S. Moodera, and G.P. Berera, *Thin Solid Films* 510, 247 (2006).
23. M. Kundakçi, B. Gürbulak, S. Doğan, A. Ateş, and M. Yildirim, *Appl. Phys. A* 90, 479 (2008).
24. K.S. Urmila, T.A. Namitha, R.R. Philip, and B. Pradeep, *Appl. Phys. A* 120, 675 (2015).
25. M.M. El-Nahass, A.-B.A. Saleh, A.A.A. Darwish, and M.H. Bahlol, *Opt. Commun.* 285, 1221 (2012).
26. A. Mohan, J. Suthagar, and T. Mahalingam, in *Proceedings of International Conference on Nanomaterials Applications and Properties*, vol 2 (2013), p. 01NTF07-11.
27. J.F. Sánchez-Royo, A. Segura, O. Lang, E. Schaar, C. Pettenkofer, L. Roa, and A. Chevy, *J. Appl. Phys.* 90, 2818 (2001).
28. X. Li, B. Xu, G. Yu, L. Xue, and L. Yi, *J. Appl. Phys.* 113, 203502 (2013).
29. C.H. Ho, Y.C. Chen, and C.C. Pan, *J. Appl. Phys.* 115, 033501 (2014).
30. A.A.A. Darwish, M.M. El-Nahass, and A.E. Bekheet, *J. Alloys Compd.* 586, 142 (2014).
31. R. Anuroop and B. Pradeep, *J. Alloys Compd.* 702, 432 (2017).
32. A.F. Qasrawi and S.R. Shehada, *Phys. E* 103, 151 (2018).
33. J. Hossain, M. Julkarnain, K.S. Sharif, and K.A. Khan, *Int. J. Renew. Energy Technol Res.* 2, 220 (2013).
34. C. Viswanathan, G.G. Rusu, S. Gopal, D. Mangalaraj, and SaK Narayandass, *J. Optoelectron. Adv. Mater.* 7, 705 (2005).
35. ASh Abdinov, R.F. Babaeva, YaG Gasanov, N.A. Ragimova, and R.M. Rzaev, *Inorg. Mater.* 49, 1180 (2013).
36. M.R. Gao, Y.F. Xu, J. Jiang, and S.H. Yu, *Chem. Soc. Rev.* 42, 2986 (2013).
37. R. Lindsay, *Phys. Rev.* 84, 569 (1951).
38. J.J. Banewicz, R.F. Haidelberg, and A.H. Luxem, *J. Phys. Chem.* 65, 615 (1961).
39. P.W. Anderson, *Phys. Rev.* 79, 705 (1950).
40. V. Thanigaimani and M.A. Angadi, *Thin Solid Film* 245, 146 (1994).
41. M. Wu, Y. Xiong, N. Jiang, M. Niang, and Q. Chen, *J. Cryst. Growth* 62, 567 (2004).
42. T. Mahalingam, S. Thanikaikarasan, V. Dhanasekaran, A. Kathalingam, S. Velumani, and J.-K. Rhe, *Mater. Sci. Eng. B* 174, 257 (2010).
43. V. Nagarajan, V. Saravanakannan, and R. Chandiramouli, *Der Pharma Chemi.* 7, 84 (2015).
44. S.S. Aplesnin, L.I. Ryabinkina, O.B. Romanova, D.A. Balaev, O.F. Demidenko, K.I. Yanushkevich, and N.S. Miroshnichenko, *Phys. Sol. Stat.* 49, 2082 (2007).
45. G.V. Lashkarev, V.I. Sichkovskyi, M.V. Radchenko, P. Aleshkevych, O.I. Dmitriev, P.E. Butorin, Z.D. Kovalyuk, R. Szymczak, A. Slawska-Waniewska, N. Nedelko, R. Yakiela, A.M. Balagurov, A.I. Beskrovnyy, and W. Dobrowolski, *Semicond. Phys. Quantum Electron. Optoelectron.* 14, 263 (2011).
46. G.V. Lashkarev, V.V. Slynko, Z.D. Kovalyuk, V.I. Sichkovskyi, M.V. Radchenko, P. Aleshkevych, R. Szymczak, W. Dobrowolski, and R. Minikayev, *Mater. Sci. Eng. C* 27, 1052 (2007).
47. G.V. Lashkarev, V.I. Sichkovskyi, M.V. Radchenko, A.I. Dmitriev, V.E. Slyn'ko, E.I. Slyn'ko, Z.D. Kovalyuk, P.E.

Butorin, W. Knoff, T. Story, R. Szymczak, R. Jakieła, P. Aleshkevych, and W. Dobrowolski, *Acta phys. Pol. A* 114, 1219 (2008).
48. T.M. Pekarek, L.H. Ranger, I. Miotkowski, and A.K. Ramdas, *J. Appl. Phys.* 99, 08D511 (2006).
49. S.A. Gad, *Appl. Phys. A* 120, 349 (2015).
50. S.A. Gad and A.M. Moustafa, *Indn. J. Phys.* 90, 903 (2016).
51. A.I. Ali, A. Abdel Moez, and A.H. Ammar, *Superlattices Microstruct* 65, 285 (2014).
52. A.I. Ali, J.Y. Son, A.H. Ammar, A. Abdel Moez, and Y.S. Kim, *Results Phys.* 3, 167 (2013).
53. S.H. Wempl and M. DiDomenico Jr, *Phys. Rev. Lett.* 23, 1156 (1969).
54. K. Anshu and A. Sharma, *Optik* 127, 48 (2016).
55. S.R. Eliott, *The physics and chemistry of solids* (Chichester: Wiley, 2000).
56. A.B. Djurisic and E.H. Li, *Opt. Commun.* 157, 72 (1998).
57. A.H. Ammar, A.M. Frid, and M.A.M. Sayam, *Vacuum* 66, 27 (2002).
58. S.E. Fritz, T.W. Kelley, and C.D. Frisbie, *J. Phys. Chem. B* 109, 10574 (2005).
59. R.H. Stolen and A. Ashkin, *Appl. Phys. Lett.* 22, 294 (1973).
60. H. Tichá and L. Tichy, *J. Optoelectron. Adv. Mater.* 4, 381 (2002).
61. P. Zhou, G. You, J. Li, S. Wang, S. Qian, and L. Chen, *Opt. Express* 13, 1508 (2005).
62. A.A. Ziabari and F.E. Ghodsi, *J. Alloys Compd.* 509, 8748 (2011).
63. B. Derkowskaa, B. Sahraouia, X.N. Phua, and W. Bala, *Proceedings of SPIE—The International Society for Optical Engineering*, vol. 4412 (2001).
64. V. Gupta and A.I. Mansingh, *J. Appl. Phys.* 80, 1063 (1996).
65. S.E. Braslavsky, *Pure Appl. Chem.* 79, 293 (2007).
66. S.M. Sze, *Physics of Semiconductor Devices* (New York: Wiley, 1969).
67. A. Segura, *Crystals* 8, 206 (2018).
68. K.C. Agarwal, B. Daniel, M. Grün, P. Feinäugle, C. Klingshirn, and M. Hetterich, *Appl. Phys. Lett.* 86, 181907 (2005).